


Transient precessing domain structures in finite-size nanomagnets and inversion of magnetization

L. Friedland^{1,*} and A. G. Shagalov^{2,†}

¹*Racah Institute of Physics, Hebrew University of Jerusalem, Jerusalem 91904, Israel*

²*Institute of Metal Physics, Ekaterinburg 620990, Russian Federation*

 (Received 13 May 2021; revised 14 July 2021; accepted 27 July 2021; published 4 August 2021)

Transient (in time) uniformly precessing magnetization structures (TUPS) on finite-length ferromagnetic wires are discussed. These rotating around the wire magnetization solutions of the Landau-Lifshits-Slonczewski equation are generalizations of traveling uniformly precessing domain walls of infinite range described by Goussev *et al.* [*Phys. Rev. Lett.* **104**, 147202 (2010)] and comprise a single parameter family of magnetization profiles controlled by the precession frequency. The latter slowly varies in time resulting in passage of the magnetization structure through different evolution stages. The modulational stability of the TUPS is also discussed. An autoresonance approach using chirped frequency transverse spin polarized current is applied to initiate TUPS with a desired precession frequency. The process of complete inversion of the magnetization of the wire involving passage from spatially uniform to nonuniform and then back to uniform precessing state with opposite magnetization is analyzed.

DOI: [10.1103/PhysRevB.104.054405](https://doi.org/10.1103/PhysRevB.104.054405)

I. INTRODUCTION

Domain structures and their dynamics in nanoscale magnetic systems are attracting increased attention nowadays because they affect design and operation of magnetic-based devices having promising technological applications like the magnetic memory [1,2], sensor devices [3], and logic concepts for magnetic computing [4,5].

The miniaturization trend of magnetic samples requires studying of magnetic structures displaying new dynamical properties, which can be realized in small size nanomagnets. It is known from Brown's theorem [6] that if the size of a magnetic particle is less than some critical value, the particle appears as a single-domain object. With the increase of the size, domains of different magnetizations divided by domain walls (DW) are found (see, for example, [7]). The critical size for this transition of magnetic configuration depends on the shape of the particle and is established by the competition between magnetostatic, exchange, and anisotropy energies [6]. In a specific case of an elongated narrow cylinder-shaped particle (a segment of a "nanowire"), the critical length was found in Refs. [8,9] by analyzing the energy barrier associated with formation of the domain wall. The critical length in this case is $l_{cr} \approx \pi\delta$, where $\delta = \sqrt{A/K}$ is the DW width, and A and K are the exchange stiffness and the effective anisotropy constant, respectively. If the size of the nanoparticle is less than l_{cr} , the formation of domains is suppressed, but in the opposite case, it is preferable. For example, for Permalloy a typical value of l_{cr} is about 30 nm. This critical length was verified in experiments on switching of magnetization of nanoscale Fe islands [10], where small elongated particles

with size less than l_{cr} reversed their magnetization by coherent rotation, typical for single-domain particles. In contrast, for larger particles, a new domain was nucleated near one edge and then the associated DW propagated through the sample to reverse the magnetization. A similar complex behavior of remagnetization of nanomagnets with sizes about l_{cr} was observed in Ref. [11].

In this paper we present a theory of new domain structures when the size of nanomagnets is of order of l_{cr} or larger. The results will allow us to describe the process of inversion of magnetization in short nanomagnets and define conditions and thresholds for the inversion. We focus on the dynamics of transient (varying in time) uniformly precessing structures (TUPS) in a ferromagnetic nanowire of length l with the easy axis along \mathbf{e}_z (in the direction of the wire) in a constant external magnetic field $\mathbf{H} = H_0\mathbf{e}_z$ and generalize the results of Goussev *et al.* [12] who discovered exact precessing DW solutions of infinite range and studied their stability [13]. The analysis will be based on a one-dimensional (1D) Landau-Lifshits-Slonczewski (LLS) equation [14,15]

$$\frac{\partial \mathbf{m}}{\partial \tau} = \mathbf{h} \times \mathbf{m} + \eta \mathbf{m} \times \frac{\partial \mathbf{m}}{\partial \tau}, \quad (1)$$

where $\mathbf{m} = \mathbf{M}/M$ is the normalized magnetization, η is the Gilbert damping parameter, and

$$\mathbf{h} = \frac{\partial^2 \mathbf{m}}{\partial \xi^2} + (m_z + h_0)\mathbf{e}_z + (\mathbf{m} \times \mathbf{j}_{SC}) \times \mathbf{m}. \quad (2)$$

Here we use dimensionless time $\tau = (\gamma K/M)t$ (γ being the gyromagnetic ratio) and coordinate $\xi = z/\delta$, the normalized length of the wire is $L = l/\delta$, while $h_0 = MH_0/K$. Finally, in Eq. (2) we have included an external driving term due to transverse, oscillating, chirped frequency spin polarized current (dimensionless) $\mathbf{j}_{SC} = M\mathbf{J}_{SC}/K = 2\varepsilon \cos \varphi_d \mathbf{e}_x$, $\varphi_d = \int \omega_d(\tau) d\tau$, which will be treated as a small perturbation in

*lazar@mail.huji.ac.il

†shagalov@imp.uran.ru

the following. Excitation of large amplitude magnetic structures and the associated switching of magnetization under the action of a radio frequency driving near the ferromagnetic resonance frequency $\omega_0 = 1 + h_0$ [in dimensional units $\omega_0 = (\gamma K/M)(1 + h_0)$] was discussed in Refs. [16–19]. In our case, the driving term was added to initiate and control TUPS via *slow passage* through ω_0 followed by autoresonance in the system, the approach used recently for excitation of large amplitude magnetization waves [20,21].

A typical dynamics of complete inversion of magnetization from $m_z = +1$ to -1 in this system in simulations (using numerical approach described in [20]) is illustrated in Fig. 1, showing $m_z(\xi, \tau)$ [Fig. 1(a)] and averaged over ξ azimuthal precession frequency $\langle \partial\varphi/\partial\tau \rangle$ of the magnetization vector [Fig. 1(b)] in the case $L = 4.5$, $h_0 = -0.2$, $\varepsilon = 6 \times 10^{-3}$, $\omega_d(\tau) = \omega_0 - \alpha\tau$, $\alpha = 5 \times 10^{-4}$, $\omega_0 = 0.8$, and $\eta = 5 \times 10^{-3}$. The figure shows the emergence and evolution of the DW on a timescale of $O(1/\eta)$ accompanied by a slowly varying averaged precession frequency of the magnetic structure around \mathbf{e}_z (negative frequency means rotation in the opposite sense). We have also found in these simulations [see Fig. 1(c)] that, while m_z versus ξ at fixed times has a form of a DW, the precession frequency $\partial\varphi/\partial\tau$ is independent of a coordinate along the wire, which is the reason for using the term “uniform precession” in TUPS. In the case of typical Permalloy parameters, $A = 10^{-11}$ J/m, $K = 10^5$ J/m³, and $M = 8 \times 10^5$ A/m, our example in Fig. 1 in real physical variables corresponds to $\delta = 10$ nm, $\omega_0/2\pi = 2.8$ GHz, and amplitude of oscillations 1.5×10^{-3} T of \mathbf{J}_{SC} . Our goal in this paper is to develop a theoretical understanding of all stages of the magnetization dynamics illustrated in this example. The paper is organized as follows. We will proceed by studying undriven and undamped dynamics in the system in Sec. II. This will be followed in Sec. III by the discussion of the dynamics of TUPS due to Gilbert damping. Section IV will focus on the process of full inversion of magnetization as shown in Fig. 1, while the stability of the process will be discussed in Sec. V. Finally, Sec. VI summarizes our conclusions.

II. UNDRIVEN AND UNDAMPED DYNAMICS

The theory in the following sections will assume both dissipation and driving as small perturbations. Therefore, to zero order of the perturbation theory, we proceed by analyzing uniformly precessing solutions by neglecting the dissipation and spin polarized current drive. We write Eq. (1) for this case in spherical coordinates ($m_x = \sin\theta \cos\varphi$, $m_y = -\sin\theta \sin\varphi$, $m_z = \cos\theta$)

$$\frac{\partial^2\theta}{\partial\xi^2} - \left(\frac{\partial\varphi}{\partial\xi}\right)^2 \sin\theta \cos\theta - q \sin\theta - \frac{1}{2} \sin(2\theta) = 0, \quad (3)$$

$$\frac{\partial}{\partial\xi} \left(\frac{\partial\varphi}{\partial\xi} \sin^2\theta \right) + \frac{\partial(\cos\theta)}{\partial\tau} = 0, \quad (4)$$

where parameter $q = h_0 - \frac{\partial\varphi}{\partial\tau}$ and free boundary conditions $\partial\theta/\partial\xi = \partial\varphi/\partial\xi = 0$ at $\xi = 0, L$ are imposed. This system

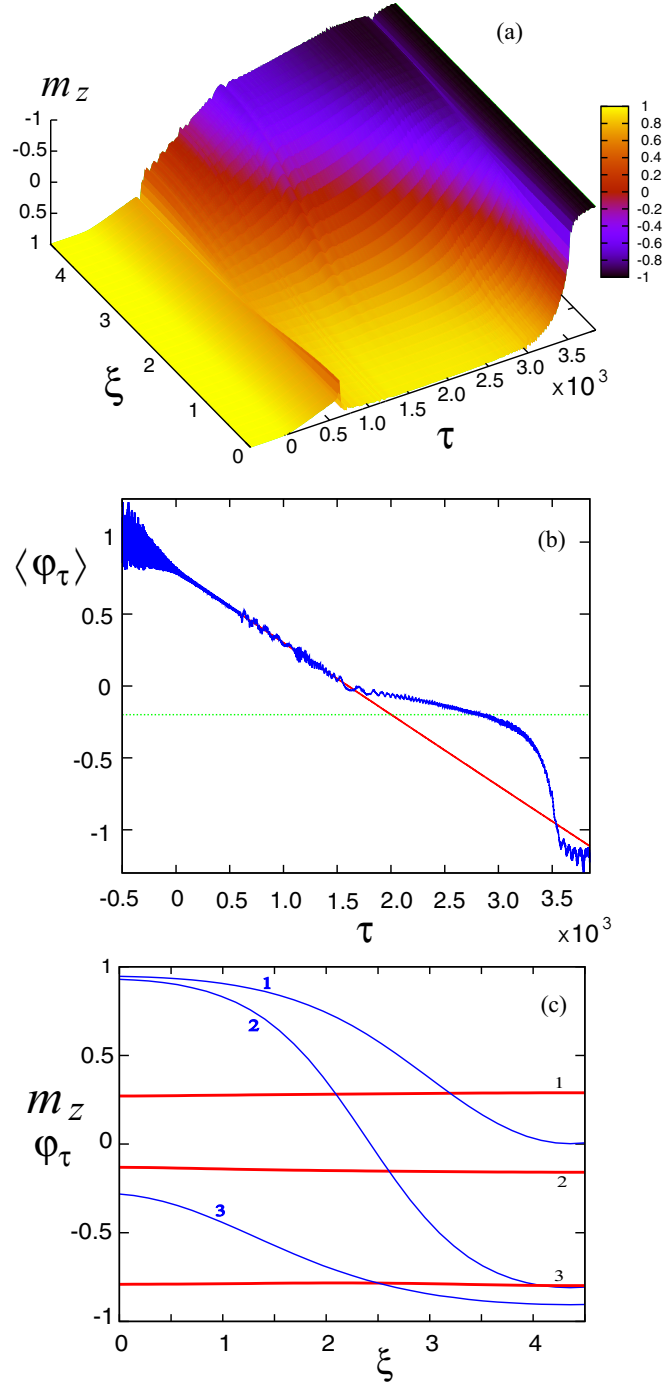


FIG. 1. Inversion of magnetization of the ferromagnetic wire driven by chirped frequency spin polarized current. The parameters are $L = 4.5$, $h_0 = -0.2$, $\varepsilon = 6 \times 10^{-3}$, $\alpha = 5 \times 10^{-4}$, $\omega_0 = 0.8$, $\eta = 5 \times 10^{-3}$. (a) Magnetization m_z versus coordinate ξ and time τ . (b) Averaged over ξ azimuthal precession frequency $\langle \varphi_\tau \rangle = \langle \partial\varphi/\partial\tau \rangle$ of magnetization vector versus τ . The straight red line in (b) is the chirped driving frequency. In part of the evolution, the precession frequency of the magnetic structure is locked to that of the drive. (c) The distribution of magnetization (blue lines) and precession frequency $\varphi_\tau = \partial\varphi/\partial\tau$ (red lines) along the wire at fixed times $\tau_1 = 1.0 \times 10^3$, $\tau_2 = 2.5 \times 10^3$, $\tau_3 = 3.5 \times 10^3$.

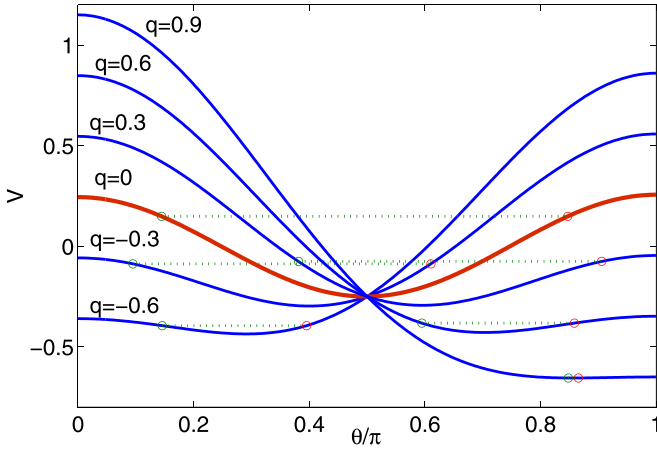


FIG. 2. Quasipotential V versus θ for several values of q . The horizontal lines correspond to the values of the quasienergy for each q . For $q = 0$ the potential (shown in red) is symmetric and describes DW having fastest descent $d\theta/d\xi$ at the bottom of the well (at $\theta = \pi/2$).

yields a family of exact uniformly precessing solutions, such that $\varphi = \omega\tau$ with constant precession frequency ω , while $\theta = \theta(\xi)$ is described by a single parameter equation

$$\frac{\partial^2 \theta}{\partial \xi^2} - q \sin \theta - \frac{1}{2} \sin(2\theta) = 0, \quad (5)$$

subject to $\partial\theta/\partial\xi = 0$ at $\xi = 0, L$, while $q = h_0 - \omega = \text{const}$.

The simplest solution of (5) is uniform $\cos \theta = -q$. Here q is defined in the whole interval $|q| < 1$, but for $L > \pi$ this solution is unstable (see Sec. V A) with respect to spatial modulations $\delta\theta, \delta\varphi \sim \cos(\kappa\xi)$, $\kappa = \pi/L$ in a smaller interval $|q| < q_r = \sqrt{1 - \kappa^2}$. However, in the region $|q| < q_r$ of instability of the uniform solution, there exists an additional *nonuniform* solution of Eq. (5). Indeed, one can write this equation as

$$\frac{\partial^2 \theta}{\partial \xi^2} = -\partial V / \partial \theta, \quad (6)$$

where $V(q, \theta) = q \cos \theta + \frac{1}{4} \cos(2\theta)$. Formally, Eq. (6) is equivalent to that describing oscillations of a particle having “coordinate” θ in the “potential well” V with ξ playing the role of “time.” This equivalence is useful in understanding spatial oscillations of θ in our system. Figure 2 illustrates $V(q, \theta)$ in the case of $L = 4.5$ for five values of $q = -0.3, 0.0, 0.3, 0.6$, and 0.9 . For these q , the potential has a local minimum $V^0 = -1/4 - q^2/2$ at $\theta = \theta^0$ satisfying $\cos \theta^0 = -q$. This θ^0 is the simplest *uniform solution* in the problem. More generally, the oscillation of θ in the potential well conserves the “energy” $A = \frac{1}{2} \dot{\theta}^2 + V$, but what is this energy for a given q ? Recall that we seek solutions satisfying the boundary conditions $\theta_\xi = 0$ at $\xi = 0, L$. This means that the ends of the wire are the “turning” points of the motion of the particle. Suppose the motion of θ proceeds from $\xi = 0$ towards the second turning point $\xi = L$. Then A must be such that half the “period” of the oscillation in the well equals L ,

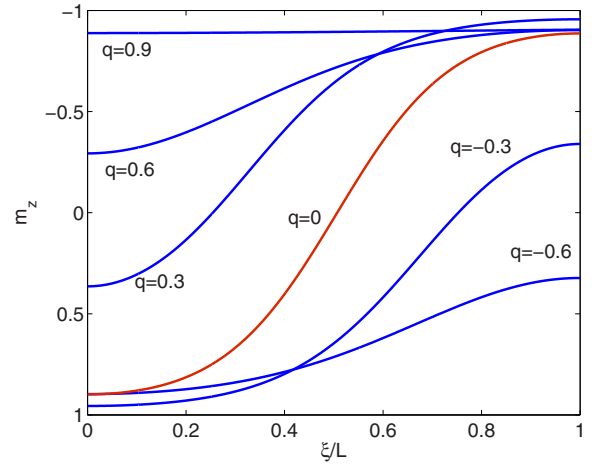


FIG. 3. The magnetization m_z versus ξ/L for each q in Fig. 2. Note that $q = 0$ case (shown in red) has the form closest to that of the precessing domain wall on an infinite wire.

i.e.,

$$\int_{\theta_1}^{\theta_2} \frac{d\theta}{\sqrt{2(A - V)}} = L, \quad (7)$$

where $\theta_{1,2}$ are the turning points given by $\cos(\theta_{1,2}) = -q \pm \sqrt{q^2 + 2A + 1/2}$. Thus, for each q (and $\omega = h_0 - q$), the boundary conditions fully define A and, consequently, find the solution $\theta(\xi, q)$ in the problem. In other words, A and the spatial form of θ become functions of two parameters L and q . In Fig. 2 these energies were found numerically via binary search using condition (7) and are shown by horizontal lines for different values of q . When the energy A , the solution $\theta(\xi, q)$ can be found from

$$\xi = \int_{\theta_1}^{\theta} \frac{ds}{\sqrt{2[A - V(q, s)]}}, \quad (8)$$

where θ_1 is one of the turning points (corresponding to $\xi = 0$, for example). Figure 3 shows the magnetization component $m_z(\xi, q) = \cos[\theta(\xi, q)]$ associated with these solutions for the values of q used in Fig. 2. These spatial magnetization structures have a form of domain walls which transform towards $m_z = -1$ as q increases.

III. DYNAMICS OF TUPS DUE TO GILBERT DAMPING

Our next step is switching on weak Gilbert damping. The damping adds two terms in the right hand side (RHS) of Eqs. (3) and (4):

$$\frac{\partial^2 \theta}{\partial \xi^2} - \left(\frac{\partial \varphi}{\partial \xi} \right)^2 \sin \theta \cos \theta - q \sin \theta - \frac{1}{2} \sin(2\theta) = \eta \frac{\partial \theta}{\partial \tau}, \quad (9)$$

$$\frac{\partial}{\partial \xi} \left(\frac{\partial \varphi}{\partial \xi} \sin^2 \theta \right) + \frac{\partial(\cos \theta)}{\partial \tau} = \eta \frac{\partial \varphi}{\partial \tau} \sin^2 \theta, \quad (10)$$

where, as before, $q = h_0 - \frac{\partial \varphi}{\partial \tau}$ and free boundary conditions $\partial\theta/\partial\xi = \partial\varphi/\partial\xi = 0$ at $\xi = 0, L$ are imposed at all times. We assume that η is a small parameter in the problem and seek solutions of form $\varphi = \int \omega(\tau) d\tau$ and $\theta = \theta_0(\tau, \xi)$, where

$\theta_0(\tau, \xi)$ and precession frequency $\omega(\tau)$ are slow, such that $\partial F/\partial \tau \sim O(\eta)$, where F is one of these functions. We also impose zero boundary conditions on $\theta_0(\tau, \xi)$. The stability of these solutions will be discussed in Sec V C.

To $O(\eta)$, Eqs. (9) and (10) become [note that by assumption $\eta\theta_{0\tau} \sim O(\eta^2)$]

$$\frac{\partial^2 \theta_0}{\partial \xi^2} - q \sin \theta_0 - \frac{1}{2} \sin(2\theta_0) = 0, \quad (11)$$

$$\frac{\partial(\cos \theta_0)}{\partial \tau} = \eta \omega \sin^2 \theta_0, \quad (12)$$

where $q = h_0 - \omega(\tau)$. Equation (11) is the same as Eq. (5), but with slow parameter $q(\tau)$ and yields solution $\theta_0(\xi)$ for each value of q . On the other hand, Eq. (12) is nontrivial by stating that for the aforementioned $\theta_0(\xi)$, ω is independent of ξ . This issue will be resolved in Sec. V B by analyzing stability of TUPS and showing that spatially dependent perturbations of $\partial\varphi/\partial\tau$ remain small. As in the time independent case above, for $|q(\tau)| \leq 1$, Eq. (11) allows a uniform but time dependent solution satisfying $\cos \theta_0 = -q(\tau)$. However, if $L > \pi$, in the subinterval $|q(\tau)| \leq q_r$ in addition to the uniform solution, there exists a nonuniform one $\theta_0(\tau, \xi)$, which can be found by solving Eq. (11) similarly to the time independent ($\eta = 0$) case above. Suppose we consider the time dependent problem with initial $|q| < q_r$ and seek time evolution of the corresponding nonuniform magnetization state. This evolution is found as follows. For each value of $q(\tau)$, one defines quasienergy $A(q) = \frac{1}{2}(\partial\theta_0/\partial\xi)^2 + V(q, \theta_0)$, where, as before, the quasipotential is $V(q, \theta_0) = q \cos \theta_0 + \frac{1}{4} \cos 2\theta_0$. This energy is found using Eq. (7) and yields the solution of $\theta_0(\tau, \xi)$ (i.e., the TUPS) via Eq. (8). But how do we find parameter $q(\tau)$ for performing these calculations? This goal is accomplished by using Eq. (12). We average this equation over ξ to get (recall the assumption of uniformity of ω discussed above)

$$\frac{d\langle \cos \theta_0 \rangle}{d\tau} = \eta \omega \langle \sin^2 \theta_0 \rangle, \quad (13)$$

where $\langle \dots \rangle = \frac{1}{L} \int_0^L (\dots) d\xi$. Importantly, the necessary condition for the decrease of $\langle \cos \theta_0 \rangle = \langle m_z \rangle$ in time is the negativity of ω . For a given q , we find θ_0 via Eq. (8) and calculate the corresponding $\langle \cos \theta_0 \rangle$ and $\langle \sin^2 \theta_0 \rangle$. Then Eq. (13) yields an ODE for $q(\tau)$,

$$\frac{dq}{d\tau} = \frac{\eta(h_0 - q)\langle \sin^2 \theta_0 \rangle}{d\langle \cos \theta_0 \rangle/dq} \quad (14)$$

and if $\omega = h_0 - q$ is negative initially, q increases (ω becomes more negative) in time continuously. Finally, as $q(\tau)$ increases, the magnetization profile becomes uniform [i.e., $\theta = \theta(\tau)$] when q passes $\sqrt{1 - (\pi/L)^2}$ at some τ . The evolution of this uniform state is described by Eq. (12) yielding an ODE:

$$\dot{\theta}_\tau = -\eta \omega \sin \theta, \quad (15)$$

where the precession frequency $\omega = h_0 + \cos \theta$. If the initial sign of ω of this uniform state is negative, θ increases continuously and the magnetization transits to $m_z = -1$.

As an example of application of our theory, Fig. 4(a) shows the evolution of the magnetization component $m_z = \cos \theta$ in

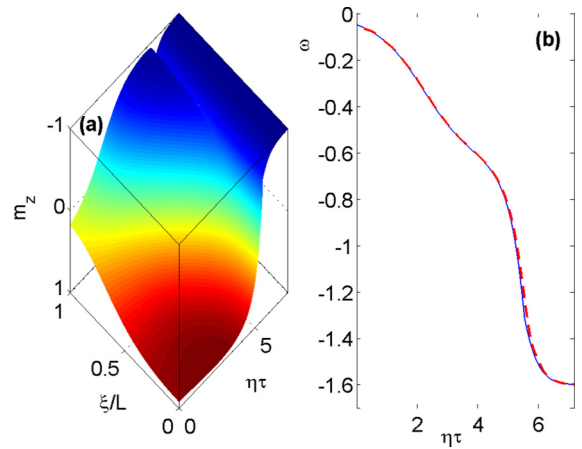


FIG. 4. (a) Magnetization m_z versus normalized time $\eta\tau$ and coordinate ξ/L . (b) Precession frequency ω in the example $L = 4.5$, $\eta = 0.05$, $h_0 = -0.6$, and initial $q = -0.55$. The red dashed line is from full numerical simulations.

the case of $L = 4.5$, $\eta = 0.05$, $h_0 = -0.6$, and initial $q = -0.55$. In addition, Fig. 4(b) illustrates the corresponding evolution of the precession frequency ω . Note that Eqs. (14) and (15) suggested using natural normalized time $T = \eta\tau$ in the figures. We have also performed full simulations using Eq. (1) in this example starting from the steady state initial magnetization profile corresponding to $q = -0.55$. The resulting m_z was the same within the resolution in Fig. 4(a). This excellent agreement between the theory and simulations is also seen in Fig. 4(b), where the precession frequency from full simulations is shown by a red dashed line.

IV. INVERSION OF MAGNETIZATION

In this section we discuss the dynamics of full inversion of magnetization of a finite-length nanowire from the initial uniform state $m_z = 1$ to -1 , as in the example shown in Fig. 1. We have shown in the previous section that slow and smooth evolution is triggered by Gilbert damping if one starts in one of the three initial magnetization states: (a) a uniform state with $|q| \leq 1$ if $L < \pi$, (b) a uniform state with $|q| > q_r = \sqrt{1 - (\pi/L)^2}$ if $L > \pi$, and (c) a nonuniform TUPS if $L > \pi$ and $|q| < q_r$. We have also shown [see Eq. (13)] that this evolution results in the decrease of $\langle \cos \theta \rangle$ (or increase of θ of the uniform state) due to the slow increase of q only if initial precession frequency ω is negative ($q > h_0$). For example, if one starts in the uniform $m_z = 1$ state and $q = -1$, this increase of θ requires $h_0 > -1$. In contrast, for positive initial ω ($q < h_0$), $\langle \cos \theta \rangle$ and ω will slowly increase, while q decreases. But how do we control the initial precessing magnetization state and prescribe parameter q (this parameter also defines the initial precession frequency $\omega = h_0 - q$)? Our idea is to invert the paradigm and instead of q , impose the precession frequency on the system, which will then define q . We exploit the autoresonance phenomenon to achieve this goal. The autoresonance approach uses a general property of many driven nonlinear systems to stay in a continuous resonance with the oscillating chirped frequency drive despite variation of the driving frequency. Under an autoresonant driving idea,

the system self-adjusts its nonlinear oscillation frequently, leading to emergence of new nonlinear states. In the past this idea was used in controlling magnetization of ferromagnetic nanoparticles [22,23] and nanowires [20,21]. Here we will use the spin polarized current drive [23] to impose the precession frequency, thereby defining the desired value of parameter q .

Assume that as in Fig. 1 one starts in $m_z = 1$ state and $L > \pi$. Then as shown in [23], if one drives the system by external chirped frequency spin polarized current of form $\mathbf{J}_{SC} = 2\varepsilon \cos \varphi_d \mathbf{e}_x$, $\varphi_d = \omega_0 \tau - \alpha \tau^2/2$, where $\omega_0 = h_0 + 1$ is the ferromagnetic resonance frequency of the ground state and slowly passes the resonance at $\tau = 0$, it enters the autoresonant precessing magnetization regime, where the precession frequency ω approximately follows the driving frequency $\omega_d = \omega_0 - \alpha \tau$. The autoresonant capture process requires the driving amplitude to exceed a threshold [23], which is the case shown in the example in Fig. 1. The precession frequency at resonance in this case is $\omega \approx \omega_0 = 0.8$ ($q = -1$) and is positive. Therefore, without the drive, the magnetization state would be frozen at $m_z = 1$ because of Gilbert damping, as described above. However, as the chirped driving continues, in autoresonance, the precession frequency locked to that of the drive will decrease and approach zero. The system will dephase from the drive at this stage because of nonadiabaticity and becomes free. If the residual precession frequency after the dephasing will be negative, the precessing state will evolve towards uniform $m_z = -1$ state, i.e., the magnetization will be fully reversed, as indeed seen in Fig. 1.

There are additional details in Fig. 1 which require further comments. During the evolution of the initial uniform state starting from $q = -1$, as $q(\tau) \approx h_0 - \omega_d(\tau)$ increases, one crosses the modulational instability point $q = -q_r$. We have found in simulations that at this time one bifurcates from uniform to a nonuniform state. At the bifurcation point, the solution develops oscillations around the smooth solution, but these oscillations are damped at later times, while averaged solution $\langle \cos \theta \rangle$ is smooth and is described well by the theory presented in the previous section. We will show later that this damping is the result of the nonuniform TUPS state being a stable attractor in the problem. After the attraction, the TUPS evolution continues, as it moves towards negative $\langle \cos \theta \rangle$ and later transforms from the nonuniform into the uniform state at $q = q_r$ and finally reaching full magnetization inversion $m_z \rightarrow -1$. We illustrate this theory in Fig. 5 showing the evolution of m_z [Fig. 5(a)] and ω [Fig. 5(b)] in the example shown in Fig. 1 in the Introduction $L = 4.5$, $h_0 = -0.2$, $\varepsilon = 6 \times 10^{-3}$, $\alpha = 5 \times 10^{-4}$, $\eta = 5 \times 10^{-3}$. Passage times of various evolution stages are indicated by numbers in Fig. 5(b). These times indicate (1) the linear resonance at $\tau = 0$ and excitation of autoresonant precessing uniform state; (2) the formation of autoresonant TUPS at $q = -q_r$; (3) the end of the autoresonant evolution when ω_d passes zero followed by free TUPS propagating due to Gilbert damping; and, finally, (4) the TUPS transforms into a uniform state, which then completes the transition to $m_z = -1$. Comparison of the results in Fig. 5(a) to those in full simulations in Fig. 1 shows that they differ by oscillations around a slowly evolving average after the transition through $q = -q_r$ and these oscillations are damped at later times. The red line in Fig. 5(b) show the results of full simula-

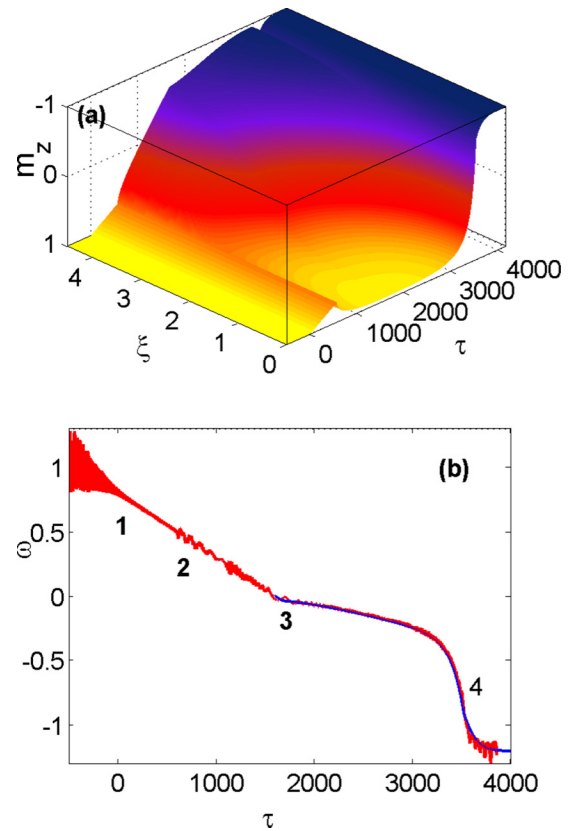


FIG. 5. The complete inversion of magnetization initiated by autoresonant drive for parameters in Fig. 1. (a) The magnetization in space-time (theory). (b) The precession frequency versus time (blue line theory, red line full simulations). The numbers indicate times of transition between different stages of evolution: 1. passage through linear resonance and excitation of autoresonant uniform state; 2. formation of autoresonant DW; 3. autoresonant evolution ends and free DW propagates due to Gilbert damping; and 4. the DW transits to uniform state, which then completes the transition to $m_z = -1$.

tions illustrating a good agreement between the theory and simulations.

V. MODULATIONAL STABILITY OF PRECESSING MAGNETIZATION STATES

In this section we consider the stability of the precessing DW solutions described above. We write $\theta = \theta_0 + \vartheta$ and $\varphi = \int \omega d\tau + \phi$, where ϑ and ϕ are small perturbations and linearize Eqs. (9) and (10) around Eqs. (11) and (12) to get

$$\begin{aligned} \frac{\partial \phi}{\partial \tau} &= -\frac{1}{\sin \theta_0} \frac{\partial^2 \vartheta}{\partial \xi^2} + \frac{G}{\sin \theta_0} \vartheta + \frac{\eta}{\sin \theta_0} \frac{\partial \vartheta}{\partial \tau}, \quad (16) \\ \frac{\partial \vartheta}{\partial \tau} &= \sin \theta_0 \frac{\partial^2 \phi}{\partial \xi^2} + 2 \frac{\partial \sin \theta_0}{\partial \xi} \frac{\partial \phi}{\partial \xi} - \eta (\sin \theta_0 \frac{\partial \phi}{\partial \tau} + \omega \cos \theta_0 \vartheta), \quad (17) \end{aligned}$$

where, as before, $\theta_0 = \theta_0(\xi, q)$, $q = h_0 - \omega$, $G = q \cos \theta_0 + \cos(2\theta_0)$, and $q(\tau)$ is a slow parameter in the problem. We will study this system in three stages of increased complexity. We proceed from $\eta = 0$ case, when θ_0 and q remain stationary and discuss stability of precessing uniform (stage A) and then

nonuniform states (stage B). Finally, in stage (C) we will include Gilbert damping and study stability of the TUPS.

A. Stability of uniform, precessing magnetization states

In $\eta = 0$ case, θ_0 and q remain constant and our linearized system is

$$\frac{\partial \vartheta}{\partial \tau} = -\frac{1}{\sin \theta_0} \frac{\partial^2 \vartheta}{\partial \xi^2} + \frac{G}{\sin \theta_0} \vartheta, \quad (18)$$

$$\frac{\partial \varphi}{\partial \tau} = \sin \theta_0 \frac{\partial^2 \phi}{\partial \xi^2} + 2 \frac{\partial \sin \theta_0}{\partial \xi} \frac{\partial \phi}{\partial \xi}, \quad (19)$$

where $G = q \cos \theta_0 + \cos(2\theta_0)$. Seeking solutions of form $\vartheta = a(\tau) \cos(\kappa \xi)$, $\phi = b(\tau) \cos(\kappa \xi)$, where $\kappa = \pi/L$, we obtain

$$[\kappa^2 + q \cos \theta_0 + \cos(2\theta_0)]a = b_\tau \sin \theta_0, \quad (20)$$

$$\kappa^2 b \sin \theta_0 + a_\tau = 0. \quad (21)$$

For the uniform solution (satisfying $\cos \theta_0 = -q$), the last two equations yield

$$a_{\tau\tau} + \kappa^2 [\kappa^2 + q \cos \theta_0 + \cos(2\theta_0)]a = 0, \quad (22)$$

predicting instability if $\kappa^2 + q \cos \theta_0 + \cos(2\theta_0) = \kappa^2 + q^2 - 1 < 0$, i.e., $|q| < q_r = \sqrt{1 - (\pi/L)^2}$ and stability in the opposite case $q_r < |q| < 1$.

B. Normal modes analysis of stability of nonuniform states

Here we start from Eqs. (16) and (17) for the perturbations, where $\theta_0 = \theta_0(\xi, q)$, $q = h_0 - \omega = \text{const.}$, and $\eta = 0$. Because of the free boundary conditions, we can *symmetrically* extend the region of definition of the perturbations ϑ and ϕ to the interval $\xi \in [-L, +L]$. Due to the symmetry around $\xi = 0$, this solution can be represented by cosine-Fourier expansions

$$\vartheta = \sum_{l=0}^N a_l(\tau) \cos(lk\xi), \quad \phi = \sum_{l=0}^N b_l(\tau) \cos(mk\xi), \quad (23)$$

which we have truncated at some N . These expansions are substituted into Eqs. (18) and (19) to get

$$\sum_{l=0}^N \frac{\partial b_l}{\partial \tau} \cos(lk\xi) = \sum_{m=0}^N \frac{(mk)^2 + G}{S} \cos(mk\xi) a_m, \quad (24)$$

$$\begin{aligned} & \sum_{l=0}^N \frac{\partial a_l}{\partial \tau} \cos(lk\xi) \\ &= - \sum_{m=0}^N mk \left[mkS \cos(mk\xi) + 2 \frac{\partial S}{\partial \xi} \sin(mk\xi) \right] b_m, \quad (25) \end{aligned}$$

where to shorten notations we defined $S = \sin \theta_0$ and $C = \cos \theta_0$. Next, we multiply (24) and (25) by $\cos(nkx)$ and average over $x \in [0, L]$ yielding in vector form

$$\frac{\partial \mathbf{b}}{\partial \tau} = \mathbf{D}^a \cdot \mathbf{a}, \quad (26)$$

$$\frac{\partial \mathbf{a}}{\partial \tau} = -\mathbf{D}^b \cdot \mathbf{b}, \quad (27)$$

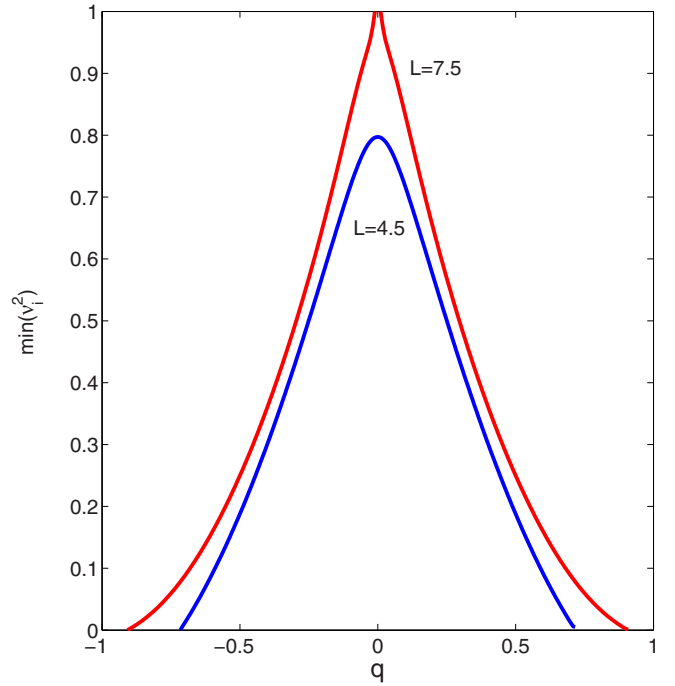


FIG. 6. Stability of nonuniform states: minimal characteristic eigenvalue $\lambda_i = v_i^2$ versus q for $L = 4.5$ and 7.5 .

where matrices \mathbf{D}^a and \mathbf{D}^b are

$$\mathbf{D}_{nm}^a = \frac{2H(n)}{L} \left[\left(\frac{(mk)^2 + G}{S} \cos(mk\xi) \cos(nk\xi) \right) \right], \quad (28)$$

$$\mathbf{D}_{nm}^b = \frac{2H(n)mk}{L} \left[\left[\frac{mkS \cos(mk\xi)}{+2 \frac{\partial S}{\partial \xi} \sin(mk\xi)} \right] \cos(nk\xi) \right], \quad (29)$$

and $H(n)$ is Heaviside function [$H(n) = 0, 0.5, 1$ for $n > 0, n = 0, n < 0$, respectively]. Finally, Eqs. (26) and (27) can be rewritten as two separate equations for \mathbf{a} and \mathbf{b} :

$$\frac{\partial^2 \mathbf{a}}{\partial \tau^2} = -\mathbf{D} \cdot \mathbf{a}, \quad \frac{\partial^2 \mathbf{b}}{\partial \tau^2} = -\tilde{\mathbf{D}} \cdot \mathbf{b}, \quad (30)$$

where $\mathbf{D} = \mathbf{D}^b \cdot \mathbf{D}^a$ and $\tilde{\mathbf{D}} = \mathbf{D}^a \cdot \mathbf{D}^b$. Note that these two equations are not independent, since, for example, in Eq. (30) for \mathbf{a} , \mathbf{b} enters via initial condition on $\partial \mathbf{a} / \partial \tau$ through Eq. (26). Seeking normal mode solutions $\mathbf{a} = \mathbf{A} \exp(-i\nu\tau)$, $\mathbf{b} = \mathbf{B} \exp(-i\tilde{\nu}\tau)$ of Eqs. (30), we have

$$(\mathbf{D} - \nu^2 \mathbf{I}) \cdot \mathbf{A} = 0, \quad (\tilde{\mathbf{D}} - \tilde{\nu}^2 \mathbf{I}) \cdot \mathbf{B} = 0. \quad (31)$$

Therefore, the stability of our system is determined by the sign of the eigenvalues $\lambda_i = \nu_i^2$ and $\tilde{\lambda}_i = \tilde{\nu}_i^2$ ($i = 1, \dots, N$) of \mathbf{D} and $\tilde{\mathbf{D}}$. We find that the two sets of the eigenvalues are the same. Furthermore, one of the eigenvalues in these sets vanishes, corresponding to $m = 0$ (spatially uniform component of the perturbation), while all the rest of the eigenvalues are positive and, therefore, our system is stable. As an illustration, Fig. 6 shows the dependence of $R = \min(\nu_i^2)$ on q found numerically in the region of existence of nonuniform states, i.e., $|q| < \sqrt{1 - (\pi/L)^2}$ for two values of $L = 4.5, 7.5$ and $N = 6$. We see that indeed in these examples R is positive indicating stability of the associated nonuniform states.

C. Stability of TUPS

Now we include Gilbert damping, so our linearized equations for the perturbations become

$$\frac{\partial \phi}{\partial \tau} = -\frac{1}{S} \frac{\partial^2 \vartheta}{\partial \xi^2} + \frac{G}{S} \vartheta + \frac{\eta}{S} \frac{\partial \vartheta}{\partial \tau}, \quad (32)$$

$$\frac{\partial \vartheta}{\partial \tau} = S \frac{\partial^2 \phi}{\partial \xi^2} + 2 \frac{\partial S}{\partial \xi} \frac{\partial \phi}{\partial \xi} - \eta \left(S \frac{\partial \phi}{\partial \tau} + \omega C \vartheta \right). \quad (33)$$

We will use the same Fourier expansions of ϑ and ϕ as above. These expansions are substituted into Eqs. (32) and (33) to get

$$\begin{aligned} & \sum_{l=0}^N \frac{\partial b_l}{\partial \tau} \cos(lk\xi) \\ &= \sum_{m=0}^N \cos(mk\xi) \left[\frac{(mk)^2 + G}{S} a_m + \frac{\eta}{S} \frac{\partial a_m}{\partial \tau} \right], \quad (34) \\ & \sum_{l=0}^N \frac{\partial a_l}{\partial \tau} \cos(lk\xi) \\ &= - \sum_{m=0}^N \left\{ mk \left[mkS \cos(mk\xi) + 2 \frac{\partial S}{\partial \xi} \sin(mk\xi) \right] b_m \right. \\ & \quad \left. + \eta \cos(mk\xi) \left(S \frac{\partial b_m}{\partial \tau} + \omega C a_m \right) \right\}. \quad (35) \end{aligned}$$

Next, we multiply (34) and (35) by $\cos(nkx)$ and average over $x \in [0, L]$ to get in vector form

$$\frac{\partial \mathbf{b}}{\partial \tau} = \mathbf{D}^a \cdot \mathbf{a} + \eta \mathbf{Q}^a \cdot \frac{\partial \mathbf{a}}{\partial \tau}, \quad (36)$$

$$\frac{\partial \mathbf{a}}{\partial \tau} = -\mathbf{D}^b \cdot \mathbf{b} - \eta \left(\mathbf{Q}^b \cdot \frac{\partial \mathbf{b}}{\partial \tau} + \mathbf{P} \cdot \mathbf{a} \right), \quad (37)$$

where matrices \mathbf{D}^a , \mathbf{D}^b are the same as above and \mathbf{Q}^a , \mathbf{Q}^b , \mathbf{P} are

$$Q_{nm}^a = \frac{2H(n)}{L} \left\langle \frac{\cos(nk\xi) \cos(mk\xi)}{S} \right\rangle, \quad (38)$$

$$Q_{nm}^b = \frac{2H(n)}{L} \langle S \cos(nk\xi) \cos(mk\xi) \rangle. \quad (39)$$

$$P_{nm} = \frac{2H(n)}{L} \omega \langle C \cos(nk\xi) \cos(mk\xi) \rangle. \quad (40)$$

Note that all these matrices are slow because of the variation of θ_0 due to the damping as described previously. Therefore, we seek an eikonal-type solution $\mathbf{a} = \mathbf{A} \exp(-i \int \nu d\tau)$, where ν is real, $\mathbf{A} = A(\tau) \mathbf{e}$, $A(\tau)$ is slow, and \mathbf{e} is the slow normalized polarization vector. Then, to $O(\eta)$, our equations can be rewritten as

$$\frac{\partial \mathbf{B}}{\partial \tau} - i\nu \mathbf{B} = \mathbf{D}^a \cdot \mathbf{A} - i\nu \eta \mathbf{Q}^a \cdot \mathbf{A}, \quad (41)$$

$$\frac{\partial \mathbf{A}}{\partial \tau} - i\nu \mathbf{A} = -\mathbf{D}^b \cdot \mathbf{B} + i\nu \eta \mathbf{Q}^b \cdot \mathbf{B} - \eta \mathbf{P} \cdot \mathbf{A}. \quad (42)$$

For nonzero ν and $\eta = 0$, from Eq. (41) we have $\mathbf{B} = \frac{i}{\nu} \mathbf{D}^a \cdot \mathbf{A}$ and by iteration in the same equation

$$\mathbf{B} = \frac{i}{\nu} \mathbf{D}^a \cdot \mathbf{A} + \frac{1}{\nu} \frac{\partial}{\partial \tau} \left(\frac{1}{\nu} \mathbf{D}^a \cdot \mathbf{A} \right) + \eta \mathbf{Q}^a \cdot \mathbf{A}, \quad (43)$$

which after substitution in Eq. (42) to $O(\eta)$ results in

$$(\mathbf{D} - \nu^2 \mathbf{I}) \cdot \mathbf{A} = i\nu \left[\frac{\partial \mathbf{A}}{\partial \tau} + \frac{\mathbf{D}^b}{\nu} \cdot \frac{\partial}{\partial \tau} \left(\frac{\mathbf{D}^a}{\nu} \cdot \mathbf{A} \right) + \eta \mathbf{Q} \cdot \mathbf{A} \right]. \quad (44)$$

Here, as before, $\mathbf{D} = \mathbf{D}^b \cdot \mathbf{D}^a$ and $\mathbf{Q} = \mathbf{D}^b \cdot \mathbf{Q}^a + \mathbf{Q}^b \cdot \mathbf{D}^a + \mathbf{P}$. Note that the right-hand side of this equation is of $O(\eta)$, suggesting the following a perturbative approach in solving the problem. We write $\mathbf{A} = \mathbf{A}_0 + \eta \mathbf{A}_1$, where \mathbf{A}_0 satisfies

$$(\mathbf{D} - \nu^2 \mathbf{I}) \cdot \mathbf{A}_0 = 0. \quad (45)$$

All matrices here are slowly varying objects due to the variation of parameter q . Equation (45) defines N slow frequencies ν_n via eigenvalues $\lambda_n = \nu_n^2$ of \mathbf{D} (these frequencies are all real as discussed above) and the corresponding normalized eigenvectors \mathbf{e}_n familiar from $\eta = 0$ limit. Then for each of these n modes, Eq. (44) yields

$$(\mathbf{D} - \nu_n^2 \mathbf{I}) \cdot \mathbf{A}_1 = i\nu_n \left[\frac{\partial \mathbf{A}_{0n}}{\partial \tau} + \frac{\mathbf{D}^b}{\nu_n} \cdot \frac{\partial}{\partial \tau} \left(\frac{\mathbf{D}^a}{\nu_n} \cdot \mathbf{A}_{0n} \right) + \eta \mathbf{Q} \cdot \mathbf{A}_{0n} \right], \quad (46)$$

where, to lowest order on the RHS of (46), $\mathbf{A}_{0n} = A_n \mathbf{e}_n$. This equation is then multiplied from the left by the left eigenvector \mathbf{e}_n^T of \mathbf{D} (eigenvector of the transposed matrix \mathbf{D}^T) corresponding to eigenvalue ν_n^2 to get

$$\mathbf{e}_n^T \cdot \left[\frac{\partial \mathbf{A}_{0n}}{\partial \tau} + \frac{\mathbf{D}^b}{\nu_n} \cdot \frac{\partial}{\partial \tau} \left(\frac{\mathbf{D}^a}{\nu_n} \cdot \mathbf{A}_{0n} \right) + \eta \mathbf{Q} \cdot \mathbf{A}_{0n} \right] = 0 \quad (47)$$

or

$$2\mathbf{e}_n^T \cdot \mathbf{e}_n \frac{\partial (\ln A_n)}{\partial \tau} = -\mathbf{e}_n^T \cdot \left[\frac{\partial \mathbf{e}_n}{\partial \tau} + \frac{\mathbf{D}^b}{\nu_n} \cdot \frac{\partial}{\partial \tau} \left(\frac{\mathbf{D}^a}{\nu_n} \cdot \mathbf{e}_n \right) + \eta \mathbf{Q} \cdot \mathbf{e}_n \right]. \quad (48)$$

Finally, we write $A_n(\tau) = A_n(0) \exp(-\int_0^\tau \delta \nu_n d\tau)$, recall that in our TUPS problem, $\frac{\partial}{\partial \tau}(\dots) = \frac{\partial}{\partial q}(\dots) \frac{dq}{dt}$, where dq/dt is given by Eq. (14) and find $\delta \nu_n$ ($-i\delta \nu_n$ is formally the imaginary correction to the zero order real frequency ν_n),

$$\delta \nu_n = \frac{\mathbf{e}_n^T \cdot \left[\frac{\partial \mathbf{e}_n}{\partial q} + \frac{\mathbf{D}^b}{\nu_n} \cdot \frac{\partial}{\partial q} \left(\frac{\mathbf{D}^a}{\nu_n} \cdot \mathbf{e}_n \right) + \eta \mathbf{Q} \cdot \mathbf{e}_n \right] \frac{dq}{dt}}{2\mathbf{e}_n^T \cdot \mathbf{e}_n}. \quad (49)$$

Obviously $\delta \nu_n$ must be positive for local stability of \mathbf{A}_n , or $-\int_0^\tau \delta \nu_n(\tau') d\tau'$ should be negative, if we follow the evolution for an extended period of time.

The same development can be performed for the azimuthal perturbation ϕ . Without further details in this case, Eqs. (36) and (37) yield the analog of Eq. (44):

$$(\tilde{\mathbf{D}} - \nu^2 \mathbf{I}) \cdot \mathbf{B} = i\nu \left[\frac{\partial \mathbf{B}}{\partial \tau} + \frac{\mathbf{D}^a}{\nu} \cdot \frac{\partial}{\partial \tau} \left(\frac{\mathbf{D}^b}{\nu} \cdot \mathbf{B} \right) \right] + \eta \tilde{\mathbf{Q}} \cdot \mathbf{B}, \quad (50)$$

where $\tilde{\mathbf{Q}} = \mathbf{D}^a \cdot \mathbf{Q}^b + \mathbf{Q}^a \cdot \mathbf{D}^b + \frac{\mathbf{D}^a}{\nu} \cdot \mathbf{P} \cdot \frac{\mathbf{D}^b}{\nu}$ and $\tilde{\mathbf{D}} = \mathbf{D}^a \cdot \mathbf{D}^b$. Again, the right-hand side of this equation is of $O(\eta)$, suggesting the same approach in solving the problem. We write $\mathbf{B} = \mathbf{B}_0 + \eta \mathbf{B}_1$, where \mathbf{B}_0 satisfies

$$(\tilde{\mathbf{D}} - \nu^2 \mathbf{I}) \cdot \mathbf{B}_0 = 0. \quad (51)$$

This equation yields N slow frequencies ν_n via eigenvalues $\lambda_n = \nu_n^2$ of $\tilde{\mathbf{D}}$ (the same as for \mathbf{D}) and corresponding normalized eigenvectors $\tilde{\mathbf{e}}_n$. Then for each of these modes, Eq. (50)

yields

$$(\tilde{\mathbf{D}} - v_n^2 \mathbf{I}) \cdot \mathbf{B}_1 = i v_n \left[\frac{\partial \mathbf{B}_{0n}}{\partial \tau} + \frac{\mathbf{D}^a}{v_n} \cdot \frac{\partial}{\partial \tau} \left(\frac{\mathbf{D}^b}{v_n} \cdot \mathbf{B}_{0n} \right) + \eta \tilde{\mathbf{Q}} \cdot \mathbf{B}_{0n} \right]. \quad (52)$$

By writing $\mathbf{B}_{0n} = B_n \tilde{\mathbf{e}}_n$ and multiplying (52) by the left eigenvector $\tilde{\mathbf{e}}_n^T$ of $\tilde{\mathbf{D}}$ we get the analog of Eq. (48):

$$2\tilde{\mathbf{e}}_n^T \cdot \tilde{\mathbf{e}}_n \frac{\partial(\ln B_n)}{\partial \tau} = -\tilde{\mathbf{e}}_n^T \cdot \left[\frac{\partial \tilde{\mathbf{e}}_n}{\partial \tau} + \frac{\mathbf{D}^a}{v_n} \cdot \frac{\partial}{\partial \tau} \left(\frac{\mathbf{D}^b}{v_n} \cdot \tilde{\mathbf{e}}_n \right) + \eta \tilde{\mathbf{Q}} \cdot \tilde{\mathbf{e}}_n \right]. \quad (53)$$

This yields the imaginary correction $-i\delta\tilde{\nu}_n = i\partial(\ln B_n)/\partial\tau$ to the frequency, where [compare to Eq. (49)]

$$\delta\tilde{\nu}_n = \frac{\tilde{\mathbf{e}}_n^T \cdot \left\{ \left[\frac{\partial \tilde{\mathbf{e}}_n}{\partial q} + \frac{\mathbf{D}^a}{v_n} \cdot \frac{\partial}{\partial q} \left(\frac{\mathbf{D}^b}{v_n} \cdot \tilde{\mathbf{e}}_n \right) \right] \frac{dq}{dt} \right\}}{2\tilde{\mathbf{e}}_n^T \cdot \tilde{\mathbf{e}}_n}. \quad (54)$$

Finally, we address the case associated with the zero mode ($v_0 = 0$). In this case, we assume that $\partial\mathbf{a}/\partial\tau$ is of $O(\eta)$, which allows to approximate Eq. (36) as

$$\frac{\partial \mathbf{b}}{\partial \tau} = \mathbf{D}^a \cdot \mathbf{a}, \quad (55)$$

showing that $\partial\mathbf{b}/\partial\tau$ is not of $O(\eta)$. We will see below that this derivative describes the correction to the precession frequency due to the initial perturbation of the solution. At this stage we substitute Eq. (55) into Eq. (37) to get

$$\frac{\partial \mathbf{a}}{\partial \tau} = -\mathbf{D}^b \cdot \mathbf{b} - \eta(\mathbf{Q}^b \cdot \mathbf{D}^a + \mathbf{P}) \cdot \mathbf{a}. \quad (56)$$

Here we seek solutions $\mathbf{a} = \mathbf{a}_0 + \eta\mathbf{a}_1$ and $\mathbf{b} = \mathbf{b}_0 + \eta\mathbf{b}_1$ where \mathbf{a}_0 and \mathbf{b}_0 are the amplitudes of the zero modes in $\eta = 0$ case. Then to lowest significant order $O(\eta)$,

$$\frac{\partial \mathbf{b}_0}{\partial \tau} = \mathbf{D}^a \cdot \mathbf{a}_0, \quad (57)$$

$$\frac{\partial \mathbf{a}_0}{\partial \tau} = -\mathbf{D}^b \cdot \mathbf{b}_0 - \eta \mathbf{D}^b \cdot \mathbf{b}_1 - \eta(\mathbf{Q}^b \cdot \mathbf{D}^a + \mathbf{P}) \cdot \mathbf{a}_0. \quad (58)$$

Next, by multiplying (58) by \mathbf{D}^a from the left, we get

$$\mathbf{D}^a \cdot \frac{\partial \mathbf{a}_0}{\partial \tau} = -\eta \tilde{\mathbf{D}} \cdot \mathbf{b}_1 - \eta \mathbf{R} \cdot \mathbf{a}_0, \quad (59)$$

where, as before, $\tilde{\mathbf{D}} = \mathbf{D}^a \cdot \mathbf{D}^b$ and $\mathbf{R} = \mathbf{D}^a \cdot (\mathbf{Q}^b \cdot \mathbf{D}^a + \mathbf{P})$. Finally, the last equation is multiplied from the left by the zero left eigenvector $\tilde{\mathbf{e}}_0^T$ of $\tilde{\mathbf{D}}$ corresponding to its zero eigenvalue, yielding

$$\tilde{\mathbf{e}}_0^T \cdot \mathbf{D}^a \cdot \frac{\partial \mathbf{a}_0}{\partial \tau} = -\eta \tilde{\mathbf{e}}_0^T \cdot \mathbf{R} \cdot \mathbf{a}_0. \quad (60)$$

In this equation we write $\mathbf{a}_0 = A_0(\tau)\mathbf{e}_0$ and calculate the imaginary frequency correction $-i\delta\nu_0 = i\partial(\ln A_0)/\partial\tau$ of the zero mode, where

$$\delta\nu_0 = \frac{\tilde{\mathbf{e}}_0^T \cdot (\mathbf{D}^a \cdot \frac{\partial \mathbf{e}_0}{\partial q} \frac{dq}{dt} + \eta \mathbf{R} \cdot \mathbf{e}_0)}{\tilde{\mathbf{e}}_0^T \cdot \mathbf{D}^a \cdot \mathbf{e}_0}. \quad (61)$$

Finally, we return to Eq. (57), where $\mathbf{b}_0 = B_0(\tau)\tilde{\mathbf{e}}_0$. Since $m = 0$ column of matrix $\tilde{\mathbf{D}}_{m,n}$ vanishes, while other elements of the matrix are not, the $m = 0$ component of $\tilde{\mathbf{e}}_0$ is unity, while all other components vanish, i.e., $\tilde{\mathbf{e}}_0$ is a constant unit vector.

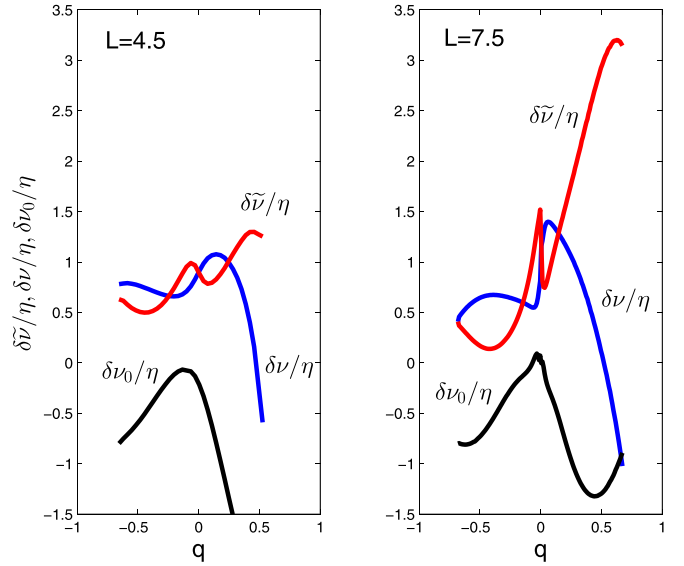


FIG. 7. Imaginary frequency corrections (relative rates of variation of the amplitudes of different modes of perturbations) $\delta\nu$, $\delta\tilde{\nu}$, and $\delta\nu_0$ versus q for $L = 4.5$, and $L = 7.5$ (in both cases $h_0 = -0.7$).

Therefore, when $\mathbf{a}_0 = A_0(\tau)\mathbf{e}_0$ is known, Eq. (57) yields the correction to the precession frequency

$$\delta\omega = \frac{\partial B_0}{\partial \tau} = A_0 \tilde{\mathbf{e}}_0 \cdot \mathbf{D}^a \cdot \mathbf{e}_0, \quad (62)$$

and since $\tilde{\mathbf{e}}_0 \cdot \mathbf{D}^a \cdot \mathbf{e}_0$ is of $O(1)$, $\delta\omega$ remains small if $A_0(\tau)$ remains small.

As an illustration of this theory, Fig. 7 shows the dependence of the imaginary frequency corrections (relative rates of variation of the amplitudes of different modes of perturbations) $\delta\nu$ and $\delta\tilde{\nu}$ vs q for the smallest nonzero frequency mode as well as $\delta\nu_0$ for the zero mode in the two examples in Fig. 6 with $L = 4.5$ and 7.5 (in both cases $h_0 = -0.7$). In most of the region of existence of the TUPS, the system is locally stable and initial perturbations $\vartheta(0, \tau)$ and $\phi(0, \tau)$ are damped on the timescale of $O(1/\eta)$. In contrast, the zero frequency mode amplitude is amplified ($\delta\nu_0 < 0$), but since the time of complete transition of TUPS is finite, a sufficiently small initial perturbation $A_0(0)$ guarantees a small departure of the magnetic structure from its slow quasisteady transient state. The case $q = 0$ (i.e., $\omega = h_0$) for a finite but long wire such that $\delta \ll L$, where δ is the width of the TUPS, is of special interest. The reason is that this TUPS is located in the middle of the wire and approximates well the $L = \infty$ case, i.e., the problem studied by Goussev *et al.* [12], suggesting stability in the latter case as well.

VI. CONCLUSIONS

We have studied a family of transient, uniformly precessing structures (TUPS) on finite-size ferromagnetic wires in the framework of a LLS equation, where Gilbert damping and chirped frequency spin polarized current driving term are viewed as small perturbations. These structures are generalizations of precessing domain walls of Goussev *et al.* [12] on an infinite domain. In the absence of damping and spin current drive, for a given normalized length L of the wire, these pre-

cessing structures are exact solutions, which do not propagate and depend on a single parameter $q = h_0 - \omega$, where h_0 is the normalized longitudinal magnetic field, ω is the precession frequency, and $|q| \leq 1$ (see Sec. II). The simplest of these solutions are uniform and stable for $L < \pi$. However, if $L > \pi$, the stability is lost in a smaller interval $|q| < \sqrt{1 - (\pi/L)^2}$ (see Sec. VA). However, in the same interval there exist additional nonuniform uniformly precessing solutions which are stable (Sec. VB).

Addition of Gilbert damping causes the aforementioned solutions to evolve and vary their precession frequency, thus affecting parameter q , which becomes a function of time. We have shown that the direction of evolution of q depends on the initial sign of the precession frequency. Negative initial ω yields the increase of q and evolution of the system towards final $m_z = -1$ state. In contrast, positive initial ω yields transition to $m_z = 1$. We have studied different scenarios of these evolutions. For example, if $L < \pi$ and initial ω is negative, the precessing solution remains uniform as it transits to $m_z = -1$. In the case $L > \pi$, if one starts in the stable nonuniform state [i.e., $|q| < \sqrt{1 - (\pi/L)^2}$] and again initial ω is negative, parameter q increases in time, the solution passes the bifurcation point $q = \sqrt{1 - (\pi/L)^2}$, becomes uniform, and reaches the $m_z = -1$ state (see illustration of this process in Fig. 4). We have also studied the stability of the transient nonuniform solutions in Sec. VC and have shown that they comprise stable attractors, i.e., the lowest frequency perturbations around these solutions are damped.

Finally, we have suggested an approach for formation of TUPS with a prescribed precession frequency. The approach exploits the autoresonance phenomenon, via small transverse

chirped frequency spin polarized current. The case of initial $m_z = 1$ is discussed in detail (see illustration in Fig. 1). We have shown that if the driving current passes the resonance with this initial uniform state, and the driving amplitude is above a threshold, it captures the system into a continuing resonance, i.e., the precession frequency of the magnetic structure follows that of the drive. This allows us to control the precession frequency of the solution and reach the desired uniformly precessing magnetization state. In the example in Fig. 1, the goal was the complete inversion of magnetization from $m_z = 1$ to -1 . The initial precession frequency in autoresonance was positive, meaning that without the drive, the system would stay in $m_z = 1$ state. However, as the autoresonance continued, both the locked driving and precession frequencies approached zero. At this stage, the system dephased from the drive because of nonadiabaticity and formed a free precessing state with small, but negative ω , which then led to full inversion of magnetization due to Gilbert damping (see the discussion of different transition stages during the process in Sec. IV).

Thus, interplay of Gilbert damping and a chirped frequency spin current drive allows us to conveniently excite and control the TUPS. Investigation of other autoresonant schemes (using microwave chirped frequency drives, for example) for excitation and control of these transient magnetic structures, seems to comprise an interesting goal for future research. Furthermore, it is known that the dissipationless and undriven LLS equation in 1D is integrable and has a large variety of solutions [9,24]. The excitation and control of some of these solutions on finite-length ferromagnetic wires and their transients under weak damping conditions comprises another important goal for the future.

-
- [1] S. S. P. Parkin, M. Hayashi, and L. Thomas, *Science* **320**, 190 (2008).
 - [2] N. Lei, T. Devolder, G. Agnus, P. Aubert, L. Daniel, J.-V. Kim, W. Zhao, T. Trypiniotis, R. P. Cowburn, C. Chappert, D. Ravelosona, and P. Lecoeur, *Nat. Nanotechnol.* **4**, 1378 (2013).
 - [3] M. Diegel, R. Mattheis, and E. Halder, *IEEE Trans. Magn.* **40**, 2655 (2004).
 - [4] P. Xu, K. Xia, C. Gu, L. Tang, H. Yang, and J. Li, *Nat. Nanotechnol.* **3**, 97 (2008).
 - [5] J. Vandermeulen, B. Van de Wiele, L. Dupre, and B. Van Waeyenberge, *J. Phys. D* **48**, 275003 (2015).
 - [6] W. F. Brown, *Phys. Rev.* **130**, 1677 (1963).
 - [7] A. Hubert and R. Schäfer, *Magnetic Domains: The Analysis of Magnetic Microstructures* (Springer, Berlin, 1998).
 - [8] H. B. Braun, *Phys. Rev. Lett.* **71**, 3557 (1993).
 - [9] H. B. Braun, *Adv. Phys.* **61**, 1 (2012).
 - [10] M. Bode, O. Pietzsch, A. Kubetzka, and R. Wiesendanger, *Phys. Rev. Lett.* **92**, 067201 (2004).
 - [11] R. P. Cowburn, D. K. Koltsov, A. O. Adeyeye, M. E. Welland, and D. M. Tricker, *Phys. Rev. Lett.* **83**, 1042 (1999).
 - [12] A. Goussev, J. M. Robbins, and V. Slastikov, *Phys. Rev. Lett.* **104**, 147202 (2010).
 - [13] Y. Gou, A. Goussev, J. M. Robbins, and V. Slastikov, *Phys. Rev. B* **84**, 104445 (2011).
 - [14] J. C. Slonczewski, *J. Magn. Magn. Mater.* **159**, L1 (1996).
 - [15] L. Berger, *Phys. Rev. B* **54**, 9353 (1996).
 - [16] H. G. Bauer, P. Majchrak, T. Kachel, C. H. Back, and G. Woltersdorf, *Nat. Commun.* **6**, 8274 (2015).
 - [17] G. Bertotti, C. Serpico, I. D. Mayergoyz, A. Magni, M. d'Aquino, and R. Bonin, *Phys. Rev. Lett.* **94**, 127206 (2005).
 - [18] W. Chen, S. H. Florez, J. A. Katine, M. J. Carey, L. Folks, and B. D. Terris, *Phys. Rev. B* **84**, 054459 (2011).
 - [19] Y. T. Cui, J. C. Sankey, C. Wang, K. V. Thadani, Z. P. Li, R. A. Buhrman, and D. C. Ralph, *Phys. Rev. B* **77**, 214440 (2008).
 - [20] L. Friedland and A. G. Shagalov, *Phys. Rev. B* **99**, 014411 (2019).
 - [21] A. G. Shagalov and L. Friedland, *Phys. Rev. E* **100**, 032208 (2019).
 - [22] G. Klughertz, P.-A. Hervieux, and G. Manfredi, *J. Phys. D: Appl. Phys.* **47**, 345004 (2014).
 - [23] G. Klughertz, L. Friedland, P.-A. Hervieux, and G. Manfredi, *Phys. Rev. B* **91**, 104433 (2015).
 - [24] A. M. Kosevich, B. A. Ivanov, and A. S. Kovalev, *Phys. Rep.* **194**, 117 (1990).